Sea spray spume droplet production in high wind speeds

F. Veron,[1] C. Hopkins,[2] E. L. Harrison,[1] and J. A. Mueller[1]

Received 1 June 2012; revised 10 July 2012; accepted 12 July 2012; published 21 August 2012.

[1] Sea spray droplets are known to enhance the fluxes of momentum, heat, and mass at the air-sea interface. Evaluating these fluxes depends in part on the so-called "spray generation function", the size distribution of droplets generated. At high wind speeds, spray is empirically observed to be plentiful near the ocean surface, however, the generation function has remained elusive both theoretically and experimentally. We report on a photographic laboratory experiment designed to directly quantify spume droplets observed at high wind speeds. The resulting sea spray concentration functions for spume droplets (diameter > 140 μm) are reported for three high wind speed conditions (31.3, 41.2, and 47.1 ms^{-1}). Our data suggest that large supra-millimeter droplets are more prevalent than previously thought. We also observed a previously unreported spray generation mechanism whereby liquid sheets form at the crests of breaking waves and generate, upon breakup, a significant number of small spume drops. **Citation:** Veron, F., C. Hopkins, E. L. Harrison, and J. A. Mueller (2012), Sea spray spume droplet production in high wind speeds, *Geophys. Res. Lett.*, *39*, L16602, doi:10.1029/2012GL052603.

1. Introduction

[2] In high wind speed conditions, it is well known that a significant amount of sea spray is generated at the surface of the ocean and gets subsequently transported in the marine atmospheric boundary layer. In turn, these spray droplets are believed to affect the multiple air-sea fluxes. Indeed, while suspended in the air, even for a short time, water droplets exchange heat, moisture, and momentum with the atmosphere and evidence suggests that a significant amount of the air-sea heat flux is carried by the sea spray [*Andreas*, 1992]. However, there is still no consensus as to the range of wind speeds over which sea spray effects cannot be neglected.

[3] In order to quantify the spray effects, an adequate knowledge of droplet physics, on a per-droplet basis, is crucial. In that regard, works by *Pruppacher and Klett* [1978] and *Andreas* [1990] have paved the way for numerous studies [e.g., *Rouault et al.*, 1991; *Andreas*, 1992; *Edson and Fairall*, 1994; *Andreas*, 1995; *Edson et al.*, 1996; *Mestayer et al.*, 1996; *Makin*, 1998; *Andreas and Emanuel*, 2001; *Van Eijk et al.*, 2001]. Yet, while droplet microphysics and dynamics are nowadays quite well understood and modeled, the source function, that is the number distribution of spray droplets generated at the ocean surface, remains elusive. This is especially true for the larger droplets which, because of their mass, fall back quickly into the ocean and may never get suspended above the wave crests, thereby evading conventional fixed height measurement techniques. These large and heavy drops, however, have the largest potential for exchanging momentum with the wind [*Andreas*, 1998]. Unfortunately, without accurate spray concentration estimates, one cannot attempt reliable projections of the total spray mediated fluxes.

[4] The largest sea spray droplets, also called spume droplets, are created when water is ripped off a wave crest by the wind [*Andreas et al.*, 1995]. Spume droplets have diameters generally larger than 40 μm and tend to form when the wind speed measured 10 m above the surface, U_{10}, reaches 7–11 ms^{-1}. The wind speed threshold depends on other surrounding conditions such as fetch and sea state [*Andreas*, 1995; *Monahan et al.*, 1983; *Mueller and Veron*, 2009].

[5] Several previous experimental studies were performed using imaging techniques to quantify sea spray droplets. For example, *Anguelova et al.* [1999] recorded videos of spume drops in a wave tank, but the resolution of their camera only allowed them to capture extremely large drops with diameters larger than 1300 μm. The imagery of *Koga* [1981] motivated the work of *Mueller and Veron* [2009] who developed a theoretical model for the spume generation functions based on the production mechanism of spume droplets through ligament formation and dislocation. While this mechanism appears to be supported by the imagery presented in this paper, we will see that the spray concentration estimates diverge somewhat from the measurements for large drops.

[6] At wind speeds higher than 20–30 ms^{-1}, such as those experienced in hurricanes, sea spray could significantly enhance the air-sea fluxes. Previously, parameterizations that were developed for low to moderate wind speed conditions had been extrapolated to higher wind speeds [*Andreas*, 1998]. Recent evidence, though, suggests that the knowledge acquired at moderate wind speeds potentially leads to inaccurate projections at higher wind speeds [*Emanuel*, 1995; *Donelan et al.*, 2004], and that a regime change in the actual physics at the air-sea surface occurs past wind speeds of 30–35 ms^{-1}.

[7] This paper reports on a high speed and high resolution photographic laboratory experiment aimed at examining the sea spray generation mechanism and measuring the spume concentration at high wind speeds where the surface waves are strongly forced.

2. Experimental Setup

[8] Experiments were performed in the high wind speed wind-wave tank in the Air-Sea Interaction Laboratory at the University of Delaware. The wind-wave tank is 7.3 m long, 0.6 m high, 0.48 m wide and made of Plexiglas (see

[1]School of Marine Science and Policy, University of Delaware, Newark, Delaware, USA.
[2]School of Earth and Atmospheric Sciences, Georgia Institute of Technology, Atlanta, Georgia, USA.

Corresponding author: F. Veron, College of Marine and Earth Studies, University of Delaware, 112C Robinson Hall, Newark, DE 19716, USA. (fveron@udel.edu)

0094-8276/12/2012GL052603

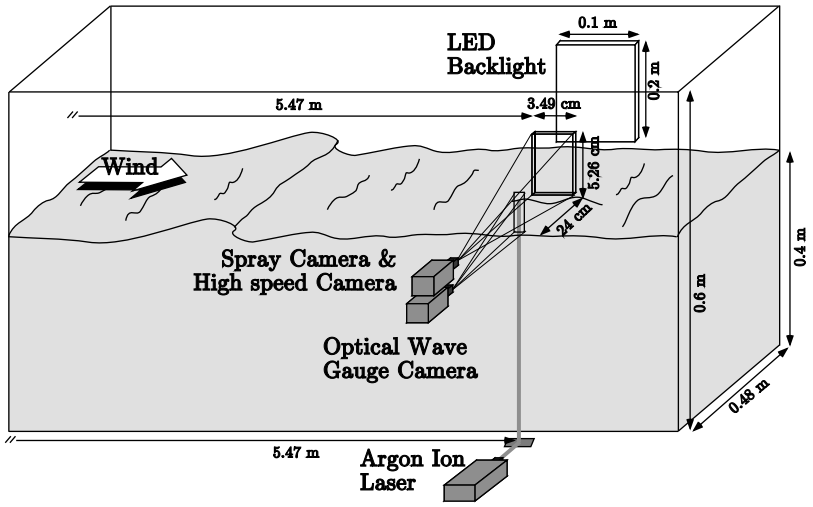

Figure 1. Schematic of the experimental setup in the small wind-wave tank at the University of Delaware's Air-Sea Interaction Laboratory.

Figure 1). The water level was maintained at 40 cm. An artificial beach was placed at the end of the tank to minimize reflected waves and dissipate wave energy.

[9] In the experiments presented here, we studied three wind speeds, U_{10} of 31.3, 41.2, and 47.1 ms^{-1}. Two distinct sets of experiments performed in fresh water are reported. We first performed a series of experiments where we used a high speed camera (Phantom 5.1) equipped with a 180 mm zoom lens and mounted on a tripod outside of the tank (Figure 1). The high speed camera acquired small frames (1000 $\times$ 1000 pixels) at a rate of 1000 Hz and with an image field of view of 6.38 cm $\times$ 6.38 cm; the crests of the waves were usually visible in the field of view. The camera was focused at a distance of 0.24 m from the back-side wall at a fetch of 5.49 m. A fluorescent backlight module was fixed to the back-side wall of the tank to provide a uniform continuous lighting. The spatial resolution in the remaining air-side of the image was not sufficient to accurately measure droplet size distributions over a satisfactory range of droplet radii. However, the high temporal resolution permitted a detailed look at the evolution of the spray generation processes and allowed us to gain insight into the physical mechanisms responsible for spray generation at these high wind speeds. A total of 10 high speed imaging segments, 4 s each, were acquired for each wind speed (see Figure 2 for example).

[10] In order to acquire reliable drop size distributions, a second series of experiments were performed using a high resolution camera (Nikon D300) equipped with a 180 mm zoom lens. The camera was mounted on a tripod perpendicular to the tank wall and took vertically oriented images (4288 $\times$ 2848 pixels) in the along-wind plane. This produced a field of view of 5.26 cm (vertically) by 3.49 cm (horizontally) with the bottom of the image placed 5.99 cm above the still water level. Focus depth and fetch were identical to that of the high speed imager. A 60 mA, 20 cm $\times$ 10 cm, LED light module was fixed to the back side wall of the tank to provide uniform flashed lighting. The image resolution was 12.27 μm/pix and the depth of field was 2 cm. The camera and backlight were synchronized and triggered by a pulse generator. The backlight was set in flash mode with a flash duration of 35 μs; this provided enough

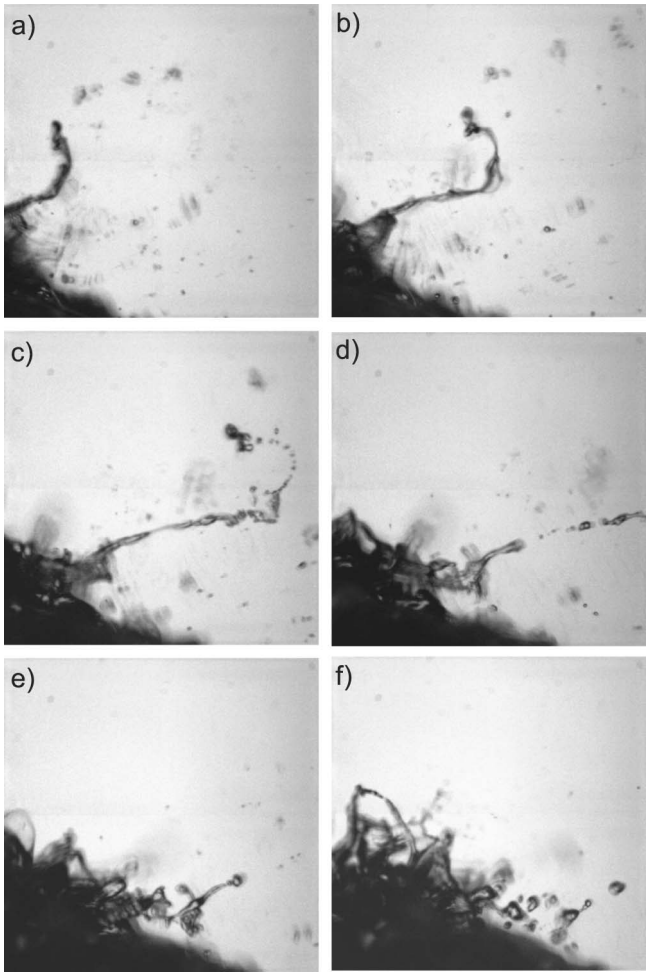

Figure 2. Images of the surface and spray generation taken with the high speed camera at a rate of 1000 fps. Each image is 6.38 cm $\times$ 6.38 cm and separated by 5 ms. The formation of a large globule/filament that subsequently fractionates into several drops is clearly visible. The 10-m equivalent wind speed is U_{10} = 31.3 ms^{-1}.

Table 1. A Summary of the 10-m Wind Speed, Friction Velocity, 10-m Neutral Drag Coefficient, Total Number of Counted Drops, and Droplet Mass Concentration in the Air, for Each of the Three Experimental Conditions

Wind Speed (U_{10} ms^{-1})	Friction Velocity (u_*)	Drag Coefficient ($C_{D_{10N}}$)	Number of Drops	Mass Concentration (kg m^{-3})
31.3	1.29	1.7×10^{-3}	3867	4.79×10^{-3}
41.2	1.98	2.3×10^{-3}	7376	7.41×10^{-3}
47.1	2.33	2.4×10^{-3}	13175	17.07×10^{-3}

illumination while being short enough to essentially freeze the drop motion, preventing smearing, and providing clear, sharp images. The experiments were done in total darkness so that the LED flashes were the sole source of illumination. For all three wind speeds, a total of 1200 images were acquired at randomly spaced time intervals to avoid imaging the same drops multiple times and to avoid aliasing with the surface wave phase. Images that captured the water surface in the picture were not processed. This occurred at the highest wind speed in 3.4% of the images and at the lowest wind speed in 1.8% of the images. After some simple binarizing (at 97% brightness level), the drops, which then appear clearly, are measured and counted. Drops with an area of less than 100 pixels yielded significant error in measuring the radius and were thus discarded. This corresponds to drops with diameters less than approximately 140 μm. The total number of drops detected in the 1200 analyzed images for each wind speed is given in Table 1.

[11] Finally, a Pitot tube and pressure transducer were placed just downwind of the imager's field of view to determine the reference wind speed profile. Measurements were taken five times each at heights of 8, 8.5, 9, and 9.5 cm above the still water surface at 200 Hz for 90 s and averaged for each height and wind speed. Those mean wind speed values as a function of height were fitted with the law of the wall to extrapolate U_{10} values, friction velocity, u_*, and drag coefficient, $C_{D_{10N}}$. These extrapolated values are used for practical comparison to other laboratory and field measurements and are shown in Table 1. Also, an optical wave gauge with which the surface elevation can be detected, was placed 2 cm upstream of the drop imaging field of view. It consisted of a digital video camera (Jai-Pulnix CV-M2CL) and a 500 mW Argon ion laser whose beam was directed vertically and intersecting with the interface. The camera was working with a reduced horizontal image size such that the sampling frequency could be set at 200 Hz.

3. Results

[12] The high speed imagery was primarily used to gain insight into the physical mechanisms responsible for the generation of spume. Figure 2 shows a sequence of images separated by 5 ms taken at a wind speed of $U_{10} = 31.3$ ms^{-1}. The breaking wave front is clearly visible and propagated from left to right. On this breaking front, an elongated globule/filament appears to be ejected from the breaking front and elongated by the wind. It subsequently fractionates rapidly into numerous daughter droplets. This frequent phenomenon appears to be a dominant mechanism for spume drop generation. It is very similar to that described by *Marmottant and Villermaux* [2004] and reminiscent of the observations of *Koga* [1981] and *Anguelova et al.* [1999] which are the basis for the spray generation model of *Mueller and Veron* [2009].

[13] Also, we wish to highlight observations of a previously unreported spray generation mechanism. Figure 3 shows a series of high speed images taken at a 1 ms interval and for a wind speed of $U_{10} = 31.3$ ms^{-1}. Besides another filament that has already fractionated, the images show the formation, on the breaking front of a wave, of a sheet of water that is inflated by the airflow (indicated by the arrows). This "balloon" grows and eventually bursts creating a large

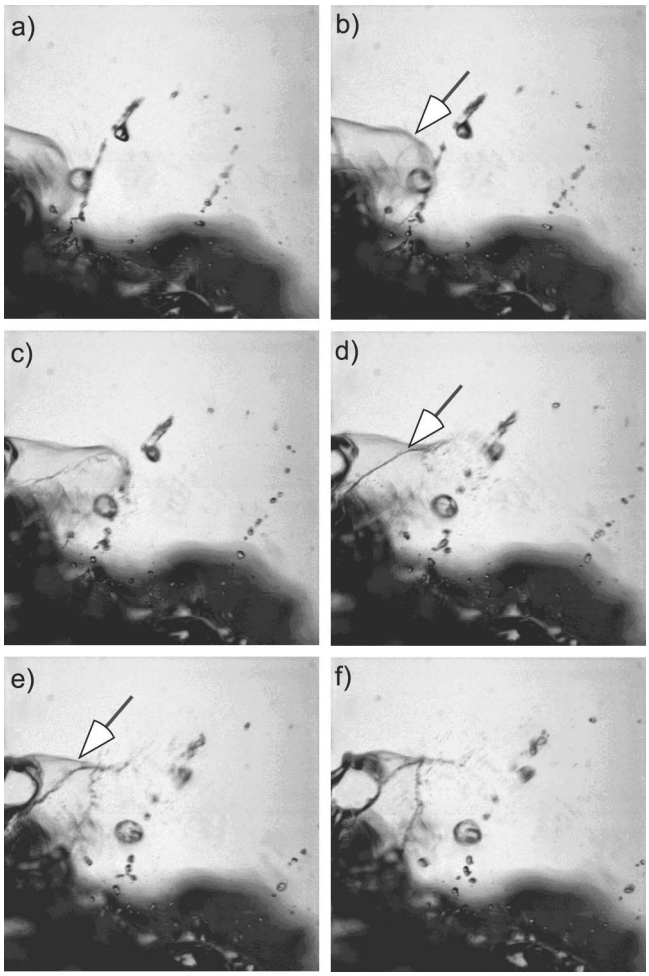

Figure 3. Images of the surface and spray generation taken with the high speed camera at a rate of 1000 fps. Each image is 6.38 cm × 6.38 cm and separated by 1 ms. The arrow shows a liquid sheet inflated by the airflow and its subsequent fractionation that yields to the generation of small water drops which are transported in the airflow. The 10-m equivalent wind speed is $U_{10} = 31.3$ ms^{-1}.

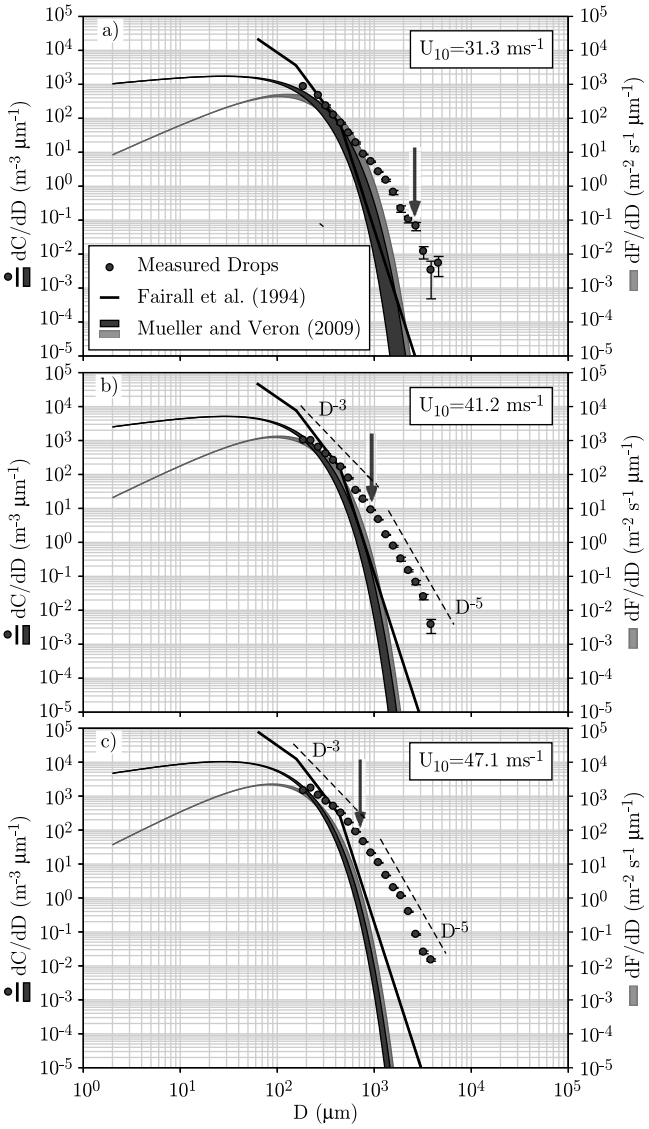

Figure 4. The spume drop concentration function dC/dD for (a) U_{10} = 31.3 ms^{-1}, (b) U_{10} = 41.2 ms^{-1}, and (c) U_{10} = 47.1 ms^{-1}. Also shown are the spray concentration functions dC/dD from *Fairall et al.* [1994] and that inferred from *Mueller and Veron* [2009]. The model of *Mueller and Veron* [2009] (thick gray lines) shows the whole range of droplets that are generated (upper range) and those that are expected to stay suspended in the airflow (lower range). For completeness, we also show the generation function dF/dD from *Mueller and Veron* [2009] (in light gray) from which dC/dD is inferred.

number of small droplets while the edge of the remaining water sheet collapses into a filament that eventually breaks as well. The breakup of liquid sheets has been extensively looked at in numerous engineering studies (see *Villermaux* [2007] for a review) but this is the first time, to the best of the authors' knowledge, that this phenomenon is observed as the result of an instability of surface waves forced by the wind. The event shown in Figure 3 is not isolated and similar events were frequently observed in the video record (at least once in each 4 s high speed video segment). We suspect that, while it is unlikely to occur in low wind speed situations, it is a recurrent occurrence in high winds and strongly forced waves such as the ones observed here at this short fetch. However, these observations of this previously unobserved physical phenomenon cover an insufficient range of wind speed and fetch conditions to establish the parameter range over which it might be significant in the generation of sea spray in high winds. Clearly, more investigations of this generation mechanism are needed.

[14] While the high speed imagery allows us to gain insight into the physics at play, the image resolution is insufficient to determine the spray size distribution over a satisfactory radii range. To this end, a second series of experiments was performed whereby high resolution digital images were taken, albeit at a much lower rate. From these images, the sea spray size distribution was determined by sorting the spray drop diameters into 20 size bins which were logarithmically spaced, with diameters centered from 196 μm to 5510 μm. The drop count in each diameter bin was then normalized by the measurement volume (3.49 cm $\times$ 5.26 cm $\times$ 2 cm) and averaged for all the images used. This led to spectral concentration function dC/dD, i.e., the number of drops per m^3 of air, per diameter increment. These concentration functions are shown in Figure 4 (symbols). Our results indicate that the drop number concentrations behave as $dC/dD \sim D^{-3}$ to $dC/dD \sim D^{-5}$ for the larger drops. The measured drop concentrations also show a significant fraction of supra-millimeter size drops which are significantly larger than the Hinze scale (indicated with the arrow), the size at which turbulent breakup dominates the fractionation process.

[15] In addition, Figure 4 shows the concentration function of *Fairall et al.* [1994], considered a relatively robust estimate, as well as the source function derived in some of our previous work [*Mueller and Veron*, 2009] (light gray) and the concentration function that can be inferred from it. The source or generation function corresponds to the spectral drop flux through the interface, i.e., number of drops generated per m^2 of sea surface per s per diameter increment. The source function is what is generally needed to estimate the spray mediated fluxes but is typically very difficult to measure. It is therefore usually either modeled or inferred from the concentration function $dF/dD = V(D)dC/dD$ where $V(D)$ is an assumed drop flux velocity (a drop generation velocity). Consequently, on Figure 4, the difference between the measured concentration (symbols) and the modeled source functions (gray area) is the generation velocity $V(D)$ that is required to reconcile the measured concentration and the modeled source function. Here, instead of using a prescribed modeled wave spectrum as in the original formulation of *Mueller and Veron* [2009], we have refined the original formulation and used the actual measurements of the wave spectrum as an input to the model. We also used $V(D)$ suggested by *Fairall et al.* [1994] to infer dC/dD from the work of *Mueller and Veron* [2009].

[16] Figure 4 shows that neither the concentration function of *Fairall et al.* [1994] nor the source function of *Mueller and Veron* [2009] appear to reproduce the observed number of very large droplets. The source function of *Mueller and Veron* [2009] clearly underestimates the production of large supra-millimeter size drops. The model of *Fairall et al.* [1994], while better, also falls short for the largest droplets measured here. In fact, one can estimate that the production velocity that can be inferred from the concentration measurements and generation function (see *Andreas et al.* [2010]

for details) leads to drop residence times and consequent ejection heights that are impossibly small (smaller than the drop size). Therefore, we find the present measurements puzzling because of the prevalence of numerous large drops that are not predicted by commonly accepted spume generation functions.

[17] A frequent spray mechanism that was observed with the high speed imaging is the formation of elongated globules or filaments on the front face of a breaking wave. These filaments subsequently break up into a number of daughter droplets. This breakup process is in fact the basis for the predictions of *Mueller and Veron* [2009] which actually fails to reproduce the large drops observed. One possible explanation for this discrepancy, which would also support the presence of large drops, is the estimation of the Hinze scale in the model. Indeed, the Hinze scale relies on estimates of the turbulent kinetic energy dissipation, which in the presence of a moving free surface and (breaking) waves can vary by several orders of magnitude in the vertical. Consequently, the Hinze scale also varies significantly with height and these measurements were done relatively close to the surface where the turbulence is expected to be somewhat reduced by the presence of the boundary. In addition, the generation of spume which is likely coincident with breaking, may be influenced by the strong alongwave horizontal modulation of the turbulence (and dissipation) when airflow separation occurs [*Veron et al.*, 2007]. Lastly, it is probable that these large drops fall back quickly and remain within a wave height of the surface. Therefore, these drops surely evade the routine spray concentration measurements that are made using fixed platforms from which most theoretical estimates are based. Despite their short lifetime, the aggregated effect of these large drops on the total air-sea momentum and heat fluxes is impossible to assess without an adequate estimate of the associated generation function.

4. Conclusion

[18] We have performed a series of laboratory experiments where both high speed and high resolution images were obtained to study, in high wind speed conditions, the sea spray generation mechanism and sea spray concentrations respectively. The observed concentration distributions of the spume reveal the presence of numerous large drops that are not accounted for in theoretical estimates of the spray generation function. The existence of these large drops could result from intermittency and local spatial variability in the near surface turbulence. Their relevance to the total air-sea fluxes remains undetermined. In addition, we also observed a previously unknown generation mechanism. Liquid sheets form at the crests of breaking waves and are subsequently inflated by the airflow. These "bubbles" eventually breakup and generate droplets with sizes at the lower range of the spume regime. This mechanism is likely to be limited to the high wind speed regime but the frequency at which it occurred in our observations suggests that it is prevalent and might need to be accounted for in estimates of spray loading and generation in hurricane or strongly forced wave conditions.

[19] **Acknowledgments.** This project was supported by NSF grants OCE-0850663 and OCE-0748767. We wish to thank anonymous reviewers whose suggestions improved the paper.

[20] The Editor thanks two anonymous reviewers for assisting in the evaluation of this paper.

References

Andreas, E. L. (1990), Time constants for the evolution of sea spray droplets, *Tellus, Ser. B*, *42*, 481–497.

Andreas, E. L. (1992), Sea spray and the turbulent air-sea fluxes, *J. Geophys. Res.*, *97*, 11,429–11,441.

Andreas, E. L. (1995), The temperature of evaporating sea spray droplets, *J. Atmos. Sci.*, *52*, 852–862.

Andreas, E. L. (1998), A new sea spray generation function for wind speeds up to 32 m/s, *J. Phys. Oceanogr.*, *28*, 2175–2184.

Andreas, E. L., and K. A. Emanuel (2001), Effects of sea spray on tropical cyclone intensity, *J. Atmos. Sci.*, *58*, 3741–3751.

Andreas, E. L., J. B. Edson, E. C. Monahan, M. P. Rouault, and S. D. Smith (1995), The spray contribution to net evaporation from the sea: A review of recent progress, *Boundary Layer Meteorol.*, *72*, 3–52.

Andreas, E. L., K. F. Jones, and C. W. Fairall (2010), Production velocity of sea spray droplets, *J. Geophys. Res.*, *115*, C12065, doi:10.1029/2010JC006458.

Anguelova, M., R. P. Barber, and J. Wu (1999), Spume drops produced by the wind tearing of wave crests, *J. Phys. Oceanogr.*, *29*, 1156–1165.

Donelan, M. A., B. K. Haus, N. Reul, W. J. Plant, M. Stiassnie, H. C. Graber, O. B. Brown, and E. S. Saltzman (2004), On the limiting aerodynamic roughness of the ocean in very strong winds, *Geophys. Res. Lett.*, *31*, L18306, doi:10.1029/2004GL019460.

Edson, J. B., and C. W. Fairall (1994), Spray droplet modeling: 1. Lagrangian model simulation of the turbulent transport of evaporating droplets, *J. Geophys. Res.*, *99*, 25,295–25,311.

Edson, J. B., S. Anquetin, P. G. Mestayer, and J. F. Sini (1996), Spray droplet modeling: 2. An interactive Eulerian–Lagrangian model of evaporating spray droplets, *J. Geophys. Res.*, *101*, 1279–1293.

Emanuel, K. A. (1995), Sensitivity of tropical cyclones to surface exchange coefficients and a revised steady-state model incorporating eye dynamics, *J. Atmos. Sci.*, *52*, 3969–3976.

Koga, M. (1981), Direct production of droplets from breaking wind waves: Its observation by a multi-colored overlapping exposure photographing technique, *Tellus*, *33*, 552–563.

Fairall, C. W., J. D. Kepert, and G. J. Holland (1994), The effect of sea spray on surface energy transports over the ocean, *Global Atmos. Ocean Syst.*, *2*, 121–142.

Makin, V. K. (1998), Air-sea exchange of heat in the presence of wind waves and spray, *J. Geophys. Res.*, *103*, 1137–1152.

Marmottant, P., and E. Villermaux (2004), On spray formation, *J. Fluid Mech.*, *498*, 73–112.

Mestayer, P. G., A. M. J. Van Eijk, G. De Leeuw, and B. S. Tranchant (1996), Numerical simulation of the dynamics of sea spray over the waves, *J. Geophys. Res.*, *101*, 20,771–20,797.

Monahan, E. C., C. W. Fairall, K. L. Davidson, and P. J. Boyle (1983), Observed inter-relations between 10 m winds, ocean whitecaps, and marine aerosols, *Q. J. R. Meteorol. Soc.*, *109*, 379–392.

Mueller, J., and F. Veron (2009), A sea state dependent spume generation function, *J. Phys. Oceanogr.*, *30*(9), 2363–2372.

Pruppacher, H. R., and J. D. Klett (1978), *Microphysics of Clouds and Precipitation*, D. Reidel, Dordrecht, Netherlands.

Rouault, M. P., P. G. Mestayer, and R. Schiestel (1991), A model of evaporating spray droplet dispersion, *J. Geophys. Res.*, *96*, 7181–7200.

Van Eijk, A. M. J., B. S. Tranchant, and P. G. Mestayer (2001), SeaCluse: Numerical simulation of evaporating sea spray droplets, *J. Geophys. Res.*, *106*, 2573–2588.

Veron, F., G. Saxena, and S. Misra (2007), Measurements of viscous tangential stresses in the separated airflow above wind waves, *Geophys. Res. Lett.*, *34*, L19603, doi:10.1029/2007GL031242.

Villermaux, E. (2007), Fragmentation, *Ann. Review Fluid Mech.*, *39*, 419–446, doi:10.1146/annurev.fluid.39.050905.110214.